

---

## Calculation and analysis of gully-buried prestressed inverted siphon structure

---

Dong-yu Ji\*

Hunan Urban Construction College,  
Xiangtan, Hunan 411101, China  
Email: dong-yu-ji@hnteuni.com  
\*Corresponding author

Xiao Mi

North China University of Water Resources and Electric Power,  
Zhengzhou, Henan 450046, China  
Email: 780643176@qq.com

**Abstract:** Inverted siphon is a kind of cross-channel building, in order to study the stress distribution law of the buried prestressed inverted siphon structure. The force and deformation characteristics of Xinanpu inverted siphon are analysed by finite element software. In the establishment of finite element calculation model, the arrangement of inverted siphon prestressed reinforcement and the setting of pier are considered. A separate reinforcement calculation model is used to simulate the effect of prestressed reinforcement by applying initial strain, the boundary condition of inverted siphon structure is simulated by the fixed constraint between inverted siphon and pier. By numerical simulation analysis of inverted siphon structure, the cloud maps of stress and displacement and path charts of inverted siphon under various cases are given, then the results are analysed to check the safety performance of inverted siphon, the research results provide a theoretical basis for construction organisation design.

**Keywords:** gully-buried inverted siphon; loss of prestress; structure design; numerical simulation; simulation analysis.

**Reference** to this paper should be made as follows: Ji, D-y. and Mi, X. (2021) 'Calculation and analysis of gully-buried prestressed inverted siphon structure', *Int. J. Critical Infrastructures*, Vol. 17, No. 1, pp.1–20.

**Biographical notes:** Dong-yu Ji received his Master in Hydraulic Structure Engineering from North China University of Water Resources and Electric Power in 2007. He is currently an Associate Professor in the Department of Building Engineering of Hunan Urban Construction College. His research interests include engineering structure simulation analysis.

Xiao Mi received her Master in Municipal Engineering from Wuhan University in 2005. She is currently a Lecturer in the School of Environmental and Municipal Engineering of North China University of Water Resources and Electric Power. Her research interests include water treatment, water technology and engineering.

---

## 1 Introduction

Inverted siphon is a kind of structure commonly used in overpass hydraulic structures, in particular, the prestressed reinforced concrete pipe in addition to the advantages of reinforced concrete pipe, its crack resistance, impermeability and resistance to longitudinal bending performance than reinforced concrete pipe (Wang et al., 2018). The prestressed reinforced concrete pipe can save a lot of steel by making full use of high strength steel bar and can bear the characteristics of high pressure water pressure. Under the same pipe diameter and water pressure, the metal content of the prestressed reinforced concrete pipe is only 10%~40% of that of the metal pipe, it is 70%~80% of the reinforced concrete pipe, besides, the pipe wall is thin, the engineering amount is small, the cost is lower than that of reinforced concrete pipe, and the seismic performance is better (Ji, 2010). But the disadvantage of inverted siphon is that the head loss is large, in the irrigation projects with precious water head, its use is limited. In addition, the navigation channels can not use the inverted siphon. Due to the high pressure head, the inverted siphon is not as convenient to use and manage as the aqueduct and other buildings (Fu et al., 2017). In operation management, also more often encountered some problems, such as joint leakage, pipe wall leakage; Longitudinal and transverse cracks occur in the pipe body; The exhaust valve is not opened in time, negative pressure will occur in the pipe; When passing the small flow, the gate is not adjusted in time, and the water jump at the pipe inlet will make the pipe body vibrate or the joint be damaged (Niu et al., 2018; Liu, 2016). The structural checking analysis of prestressed reinforced concrete pipe is carried out, considering the stress conditions under dead weight, prestress and water pressure, determine the stress and deformation of each control section, it provides the basis for evaluating the working state of the structure and selecting the reinforcement scheme.

The traditional structural mechanics method does not fully consider the interaction between the structure and the surrounding backfill and foundation in the design of inverted siphon structure, the surrounding soil is only regarded as the external load acting on the structure, but in fact, the surrounding soil exerts force on the structure, and the structural mechanics method cannot reflect the real stress situation of the structure (Peng, 2019; Zheng and Ma, 2019; Li, 2018). The inverted siphon project generally has the characteristics of long pipeline, complicated technology and huge investment, etc (Zhao, 2018). Therefore, in the model test, it is difficult to simulate according to the actual engineering scale. In the finite element analysis of inverted siphon structure, most scholars only use integral model to simulate the distribution of reinforcement in reinforced concrete, although this method cannot observe the stress and strain of the reinforcement, resulting in incomplete results (Zhang, 2018).

Due to the long inverted siphon pipe buried in soil, coupled with the constraint effect of the pier, the boundary conditions of the inverted siphon structure are complex, as a result, the distribution of stress and deformation is more complicated. In recent years, Chinese scholars have carried out extensive and in-depth studies on inverted siphon structure, but most of these research results focus on structural design, construction methods, new technology and the application of new materials, there are few research results on numerical simulation analysis of buried trench prestressed inverted siphon structure, there is a lack of deep research on the structure of inverted siphon.

## 2 Simulation of prestressed rebar and prestressed loss

In the calculation of normal limit state of prestressed concrete members, the loss of prestress due to the following factors shall be considered. Friction between the prestressed steel bar and the pipe wall is  $\sigma_{11}$ , anchorage deformation, steel retraction and joint compression is  $\sigma_{12}$ , the temperature difference between the prestressed rebar and the pedestal is  $\sigma_{13}$ , elastic compression of concrete is  $\sigma_{14}$ , stress relaxation of prestressed rebar is  $\sigma_{15}$ , shrinkage and creep of concrete is  $\sigma_{16}$  (SL191-2008, 2008).

- 1 The loss of prestress caused by friction between the prestressed rebar and the pipe wall, it can be calculated by the following formula.

$$\sigma_{11} = \sigma_{con} [1 - e^{-(\mu\theta + kx)}] \quad (1)$$

In the expression, tension control stress under anchor of prestressed reinforcement is  $\sigma_{con}$ ; coefficient of friction between prestressed rebar and pipe wall is  $\mu$ ; the sum of the included angles from the tension end to the tangent line of the pipe section curve is  $\theta$ ; influence coefficient of local deviation of pipeline per metre on friction is  $k$ ; the length of the pipe from the tension end to the calculated section is  $x$ , the projected length of the pipe on the longitudinal axis of the member can be approximated.

- 2 Prestressed linear reinforcement is caused by anchorage deformation, reinforcement retraction and joint compression, it can be calculated by the following formula.

$$\sigma_{12} = \frac{\sum \Delta l}{l} E_p \quad (2)$$

In the expression, tensile end anchorage deformation, reinforcement retraction and joint compression value is  $\Delta l$ ; the distance between the tensioning end and the anchorage end is  $l$ .

- 3 Prestress loss due to elastic compression of concrete, it can be calculated by the following formula.

$$\sigma_{14} = \alpha_{EP} \sum \Delta \sigma_{pc} \quad (3)$$

In the expression, at the centre of gravity of the section of the steel bar which is pretensioned in calculating the section, normal stress of each batch of rebar is  $\Delta \sigma_{pc}$ ; ratio of the elastic modulus of prestressed reinforcement to that of concrete is  $\alpha_{EP}$ .

- 4 The loss of prestress due to reinforcement relaxation can be calculated by the following formula.

$$\sigma_{15} = \psi \cdot \zeta \left( 0.52 \frac{\sigma_{pe}}{f_{pk}} - 0.26 \right) \sigma_{pe} \quad (4)$$

In the expression, tension coefficient is  $\psi$ , first tension is  $\psi = 1.0$ , super tension is  $\psi = 0.9$ ; relaxation coefficient of reinforcement is  $\zeta$ ; reinforcement stress during force transfer anchorage is  $\sigma_{pe}$ .

- 5 The loss of prestressed steel bars in tension zone and compression zone caused by concrete shrinkage and creep, it can be calculated by the following formula (Hu and Zhang, 2004).

$$\sigma_{16}(t) = \frac{0.9[E_p \varepsilon_{cs}(t, t_0) + \alpha_{EP} \sigma_{pc} \varphi(t, t_0)]}{1 + 15 \rho \rho_{ps}} \quad (5)$$

$$\sigma'_{16}(t) = \frac{0.9[E_p \varepsilon_{cs}(t, t_0) + \alpha_{EP} \sigma'_{pc} \varphi(t, t_0)]}{1 + 15 \rho' \rho'_{ps}} \quad (6)$$

### 3 Calculation model of inverted siphon

#### 3.1 Project summary

Xinanpu inverted siphon is an integral part of Dazhen irrigation area in Shaoyang, Hunan province. Dazheng irrigation area is located in the west of Shaoyang area, in the upper reaches of Zishui, between Yishui and Lishui. The whole project starts from the source of the Dazhen reservoir, including the Xinanpu inverted siphon pipeline, the three reservoirs of Dashuijiang, Dongfeng and Bitian. It includes 250 km of trunk canals, trunk canals and ancillary buildings, Bridges, aqueducts, tunnels, etc. It also includes 2,300 km of branch canals, connecting more than 210 small reservoirs and 30,000 dams. The irrigation area includes five counties, 12 districts, 48 towns and villages in Xinning, Wugang, Shaoyang, Longhui and Dongkou. The total area is 2,680 m<sup>2</sup>, the cultivated area is 775,900 mu. Inverted siphon design flow is 7.5 m<sup>3</sup>/s, flow velocity is 2.39 m/s, the smallest head is 78 m, design head is 90 m, head loss is 2.882 m, the total length of the inverted siphon pipe is 781.5 m. The inverted siphon adopts single hole circular pipe trench buried inverted siphon, pipe inner diameter is 2.0 m, wall thickness is 0.13 m, the pipe body adopts one-stage prestressed reinforced concrete pipe, the strength grade of concrete is C30, the grade of reinforcement shall be the second grade.

#### 3.2 Calculation model

In the numerical simulation analysis of trench embedded prestressed inverted siphon structure, The finite element model of inverted siphon structure is established (Wang, 2003). SOLID45 is adopted to simulate the pipe body, cushion, ballast and surrounding rock; The prestressed bar was simulated by link element LINK8 (Ren, 2003). Inverted siphon and bedrock calculation model is shown in Figure 1, finite element analysis model of inverted siphon is shown in Figure 2.

#### 3.3 Material parameters and cases

The concrete elastic modulus of the inverted siphon and the ballast piers is 34.5 GPa, bulk weight is 2,500 kg/m<sup>3</sup>, Poisson's ratio is 0.167; The elastic modulus of concrete cushion is 30 GPa, bulk weight is 2,450 kg/m<sup>3</sup>, Poisson's ratio is 0.2; the elastic modulus of prestressed reinforcement is 200 GPa, bulk weight is 7,850 kg/m<sup>3</sup>, Poisson's ratio is

0.28; the elastic modulus of surrounding rock is 15 GPa, bulk weight is 2,400 kg/m<sup>3</sup>, Poisson's ratio is 0.28.

**Figure 1** Inverted siphon and bedrock calculation model (see online version for colours)

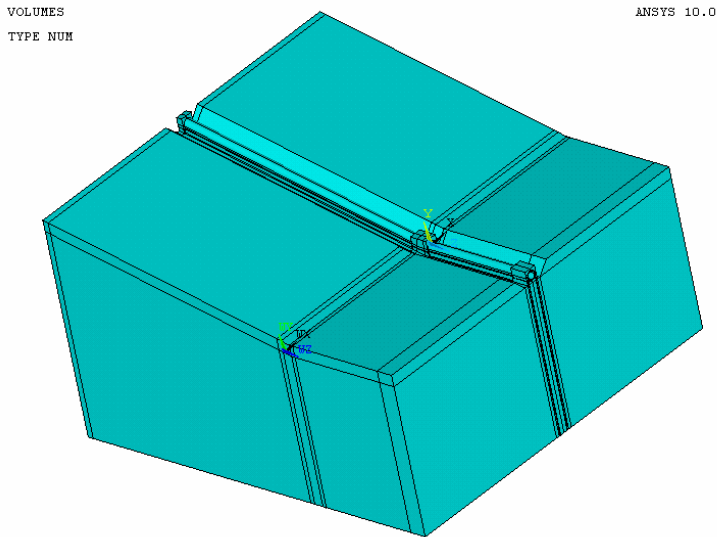
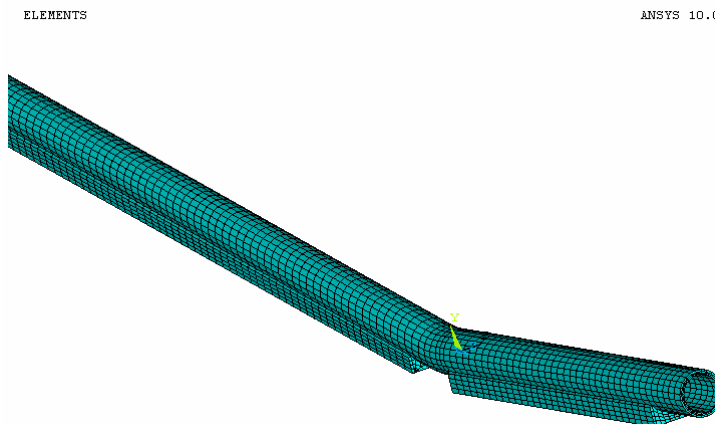


**Figure 2** Finite element analysis model of inverted siphon (see online version for colours)



According to the stress characteristics of trench embedded prestressed inverted siphon structure during construction and operation, the following four cases are mainly considered in the calculation as follows (Li et al., 2006). Inverted siphon weight is considered in case 1; Inverted siphon weight and prestressed are considered in case 2; Inverted siphon weight, prestressed and the smallest water head are considered in case 3; Inverted siphon weight, prestressed and the design water head are considered in case 4.

The numerical simulation model of the buried inverted siphon structure was established with finite element software. Considering the construction and operation characteristics of the buried inverted siphon structure, the corresponding boundary

conditions were applied. A separate reinforcement model is adopted to simulate the effect of prestressed reinforcement. According to the stress characteristics of inverted siphon structure during construction and operation, the calculation condition of structure analysis is determined. Through numerical simulation, the stress and deformation distribution of inverted siphon structure are given.

#### 4 Structure analysis of inverted siphon

In order to carry out numerical simulation analysis on the inverted siphon of the buried ditch, the stress and deformation distribution of inverted siphon structure are studied. The stress distribution of the inverted siphon and the surrounding soil in all directions and the main stress distribution cloud maps are studied, and the circumferential and axial stress cloud maps of inverted siphon prestressed reinforcement under various working conditions are studied. By defining the analysis path, the stress curve of the inverted siphon analysis path is studied. The deformation analysis mainly studies the displacement distribution of inverted siphon and surrounding soil.

##### 4.1 Stress cloud map

Through the finite element simulation analysis of trench embedded prestressed inverted siphon structure, the stress distribution cloud map of inverted siphon under four cases is obtained, they are shown from Figure 3 to Figure 14.

**Figure 3** The longitudinal stress cloud map of inverted siphon under case 1(Pa) (see online version for colours)

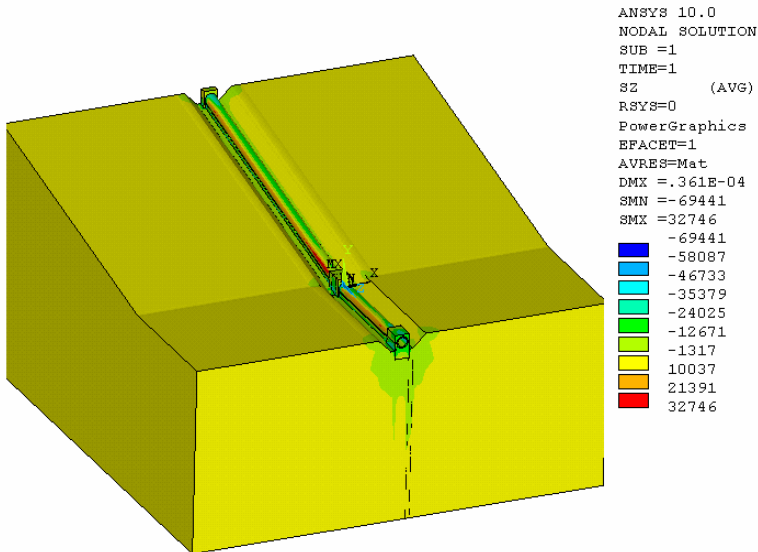


**Figure 4** The first principal stress cloud map of inverted siphon under case 1(Pa) (see online version for colours)

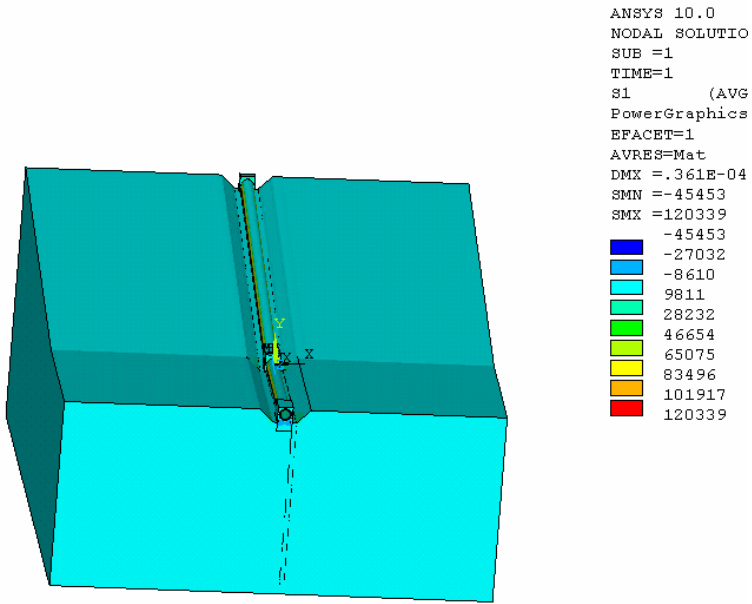


**Figure 5** The vertical stress cloud map of inverted siphon under case 2(Pa) (see online version for colours)

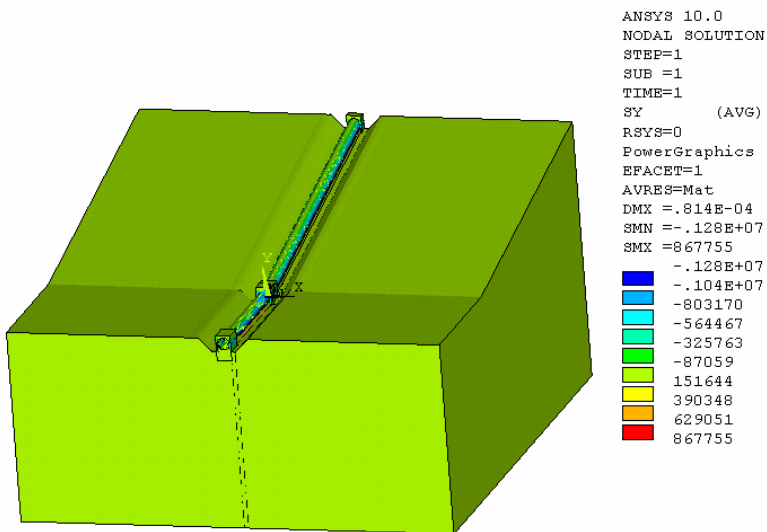


**Figure 6** The first principal stress cloud map of inverted siphon under case 2(Pa) (see online version for colours)

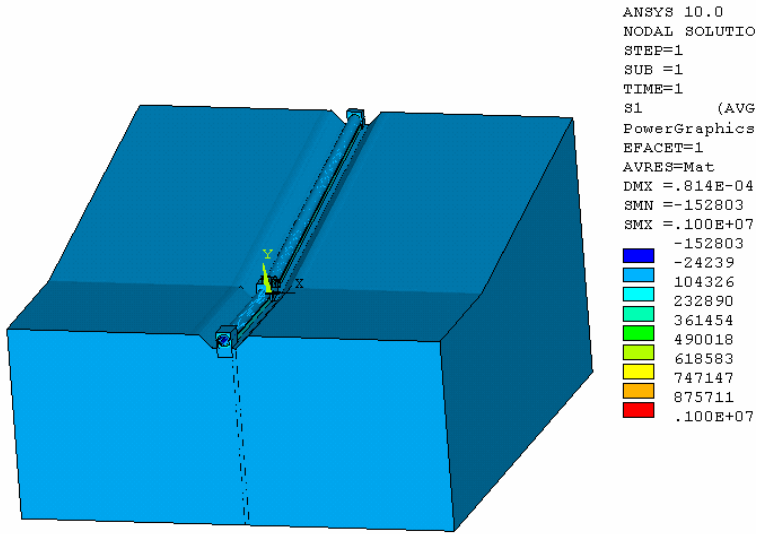


**Figure 7** The transverse stress cloud map of inverted siphon under case 3(Pa) (see online version for colours)

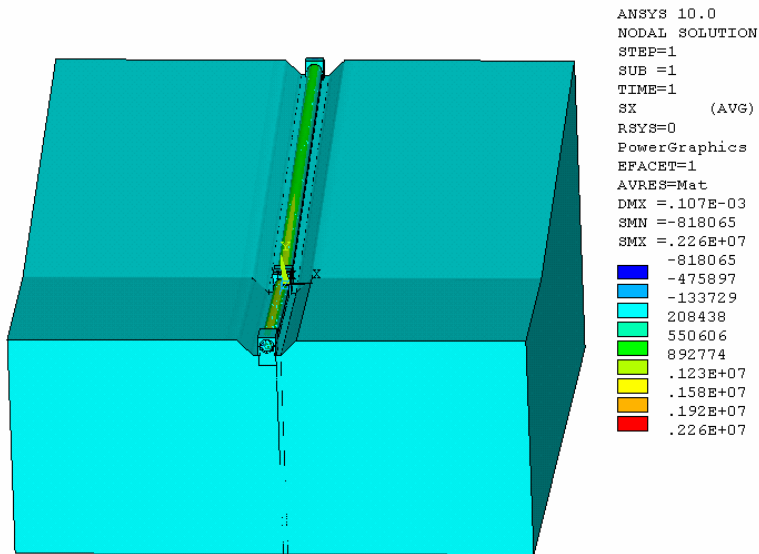




**Figure 8** The first principal stress cloud map of inverted siphon under case 3(Pa) (see online version for colours)

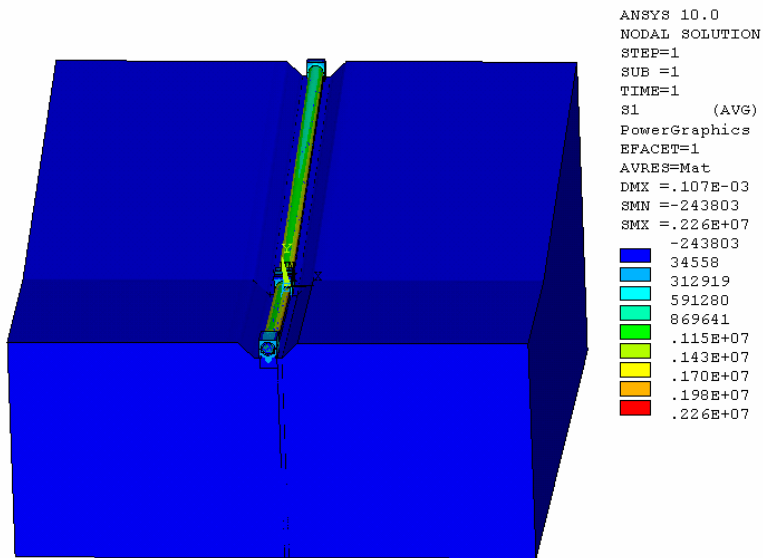


**Figure 9** The vertical stress cloud map of inverted siphon under case 4(Pa) (see online version for colours)

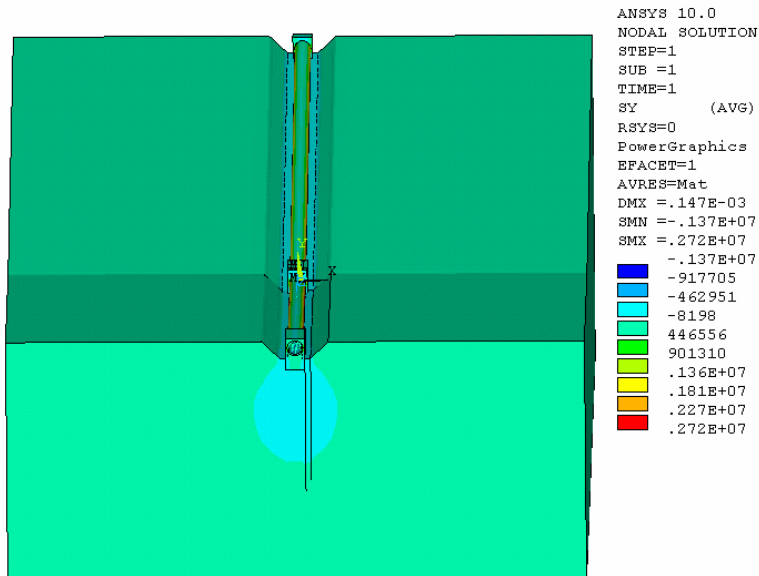


**Figure 10** The first principal stress cloud map of inverted siphon under case 4(Pa) (see online version for colours)

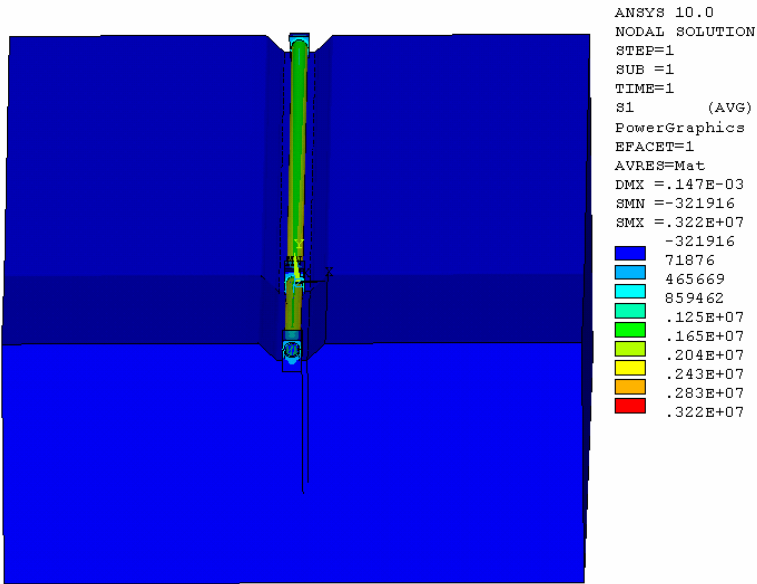


**Figure 11** The circumferential stress cloud map of prestressed reinforcement under case 3(Pa) (see online version for colours)

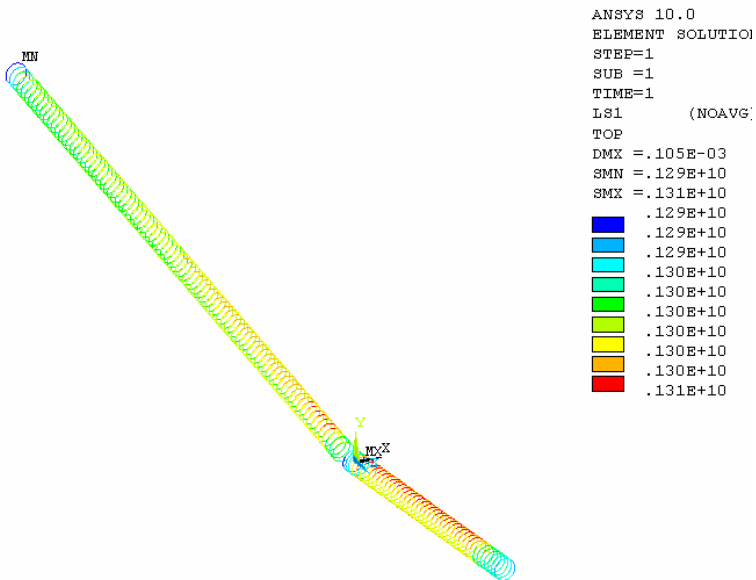


**Figure 12** The axial stress cloud map of prestressed reinforcement under case 3(Pa) (see online version for colours)

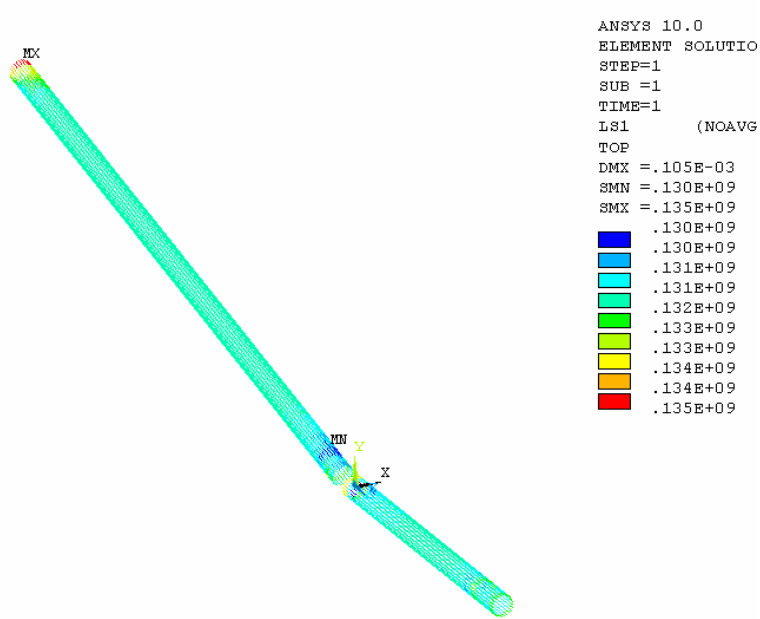
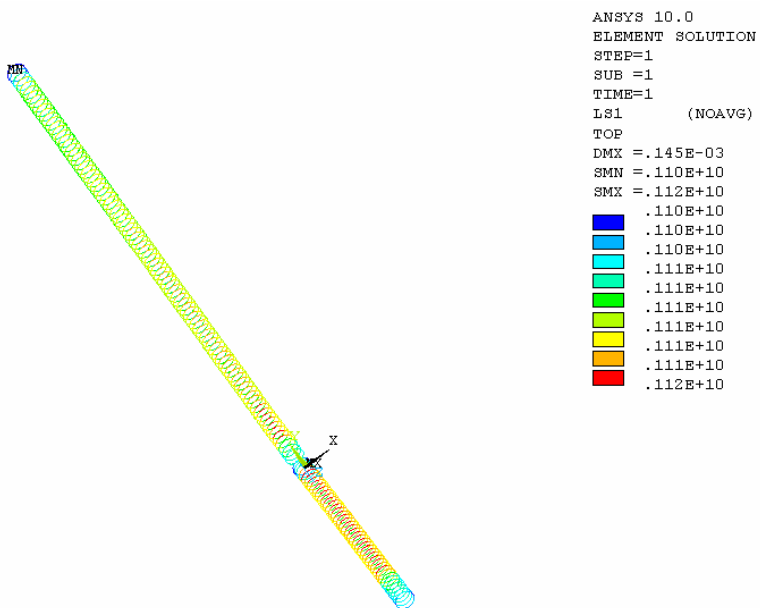


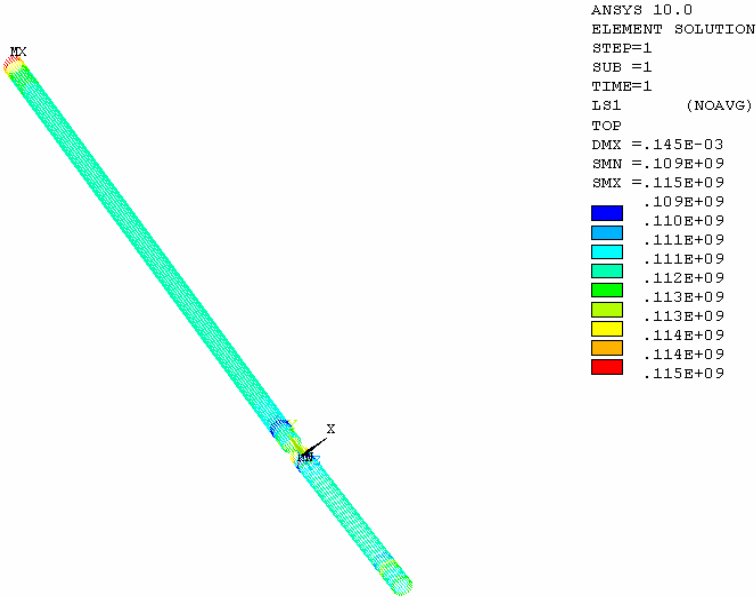
**Figure 13** The circumferential stress cloud map of prestressed reinforcement under case 4(Pa) (see online version for colours)



As can be seen from the stress analysis results, under case 1, the maximum tensile stress of the structure is 120.339 kPa, less than 1.43 MPa, which meets the requirements of the

design specification. Under case 2, the maximum tensile stress of inverted siphon is 1 MPa, and the maximum stress is less than the designed value of crack strength of C30 concrete. Therefore, the inverted siphon will not produce cracks under the action of dead weight and prestress. The vertical displacement of inverted siphon after prestressing is smaller than that before prestressing. In this case, the structure meets the requirements of bearing capacity, normal use and crack resistance. Under case 3, the maximum tensile stress of inverted siphon is 2.26 MPa, and a small range of stress concentration occurs, but the structure will not produce obvious cracks, the compressive stress was far less than 14.3 MPa, meeting the requirements. The maximum tensile stress of inverted siphon is 3.22 MPa, since the stress concentration occurs at the junction of pipe, at the junction, the ballast block is fixed to ensure the safety of its use, and the structure will not produce obvious cracks.

**Figure 14** The axial stress cloud map of prestressed reinforcement under case 4(Pa) (see online version for colours)



Under the smallest water head and design water head, the circumferential stress of prestressed rebar is 1,310 MPa and 1,120 MPa respectively, the axial stress was 135 MPa and 115 MPa respectively. The stress is within the allowable range of the reinforcement, the stress of annular reinforcement is greater than that of axial reinforcement, because the circumferential reinforcement is mainly subjected to the action of internal water pressure. The use of prestressed bars can increase the carrying capacity of the inverted siphon, which is a common form of inverted siphon.

*4.2 Stress of analysis path*

In order to study the stress change of inverted siphon on a specific path under various cases, the analysis path is defined, the inside surface of the inverted siphon is taken from the top of the pipe to the bottom of the pipe, and the path is defined clockwise. Inverted

siphon in various cases, stress change curves on different analysis paths are shown from Figure 15 to Figure 22.

**Figure 15** The transverse stress change curve of path under case 1(Pa) (see online version for colours)

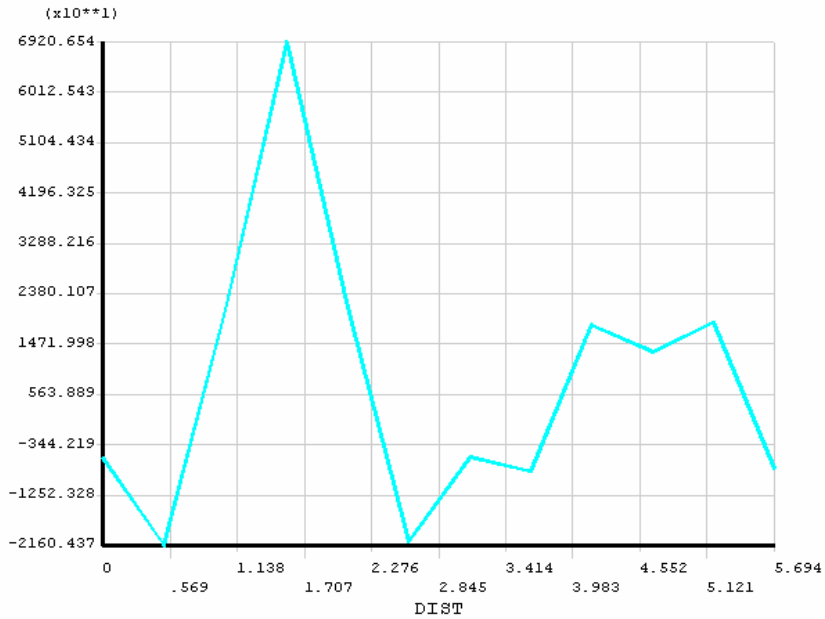


**Figure 16** The first principal stress change curve of path under case 1(Pa) (see online version for colours)

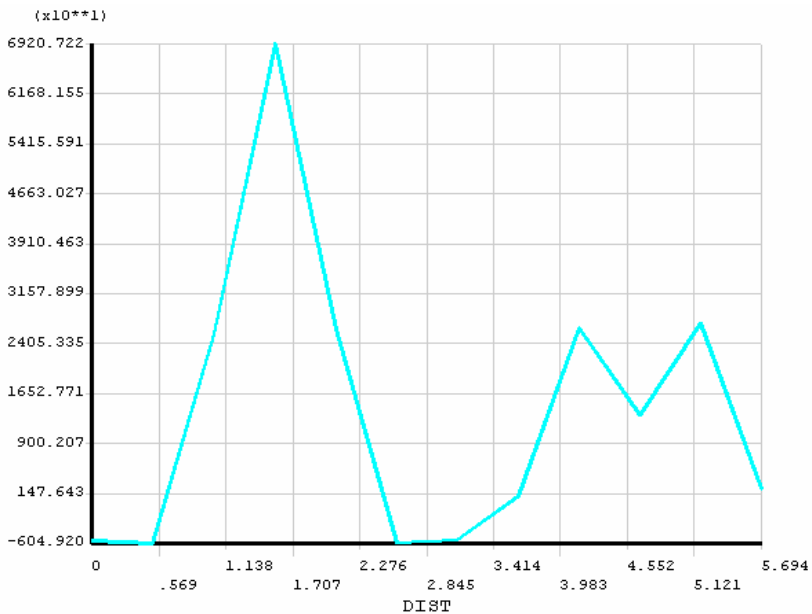


**Figure 17** The transverse stress change curve of path under case 2(Pa) (see online version for colours)

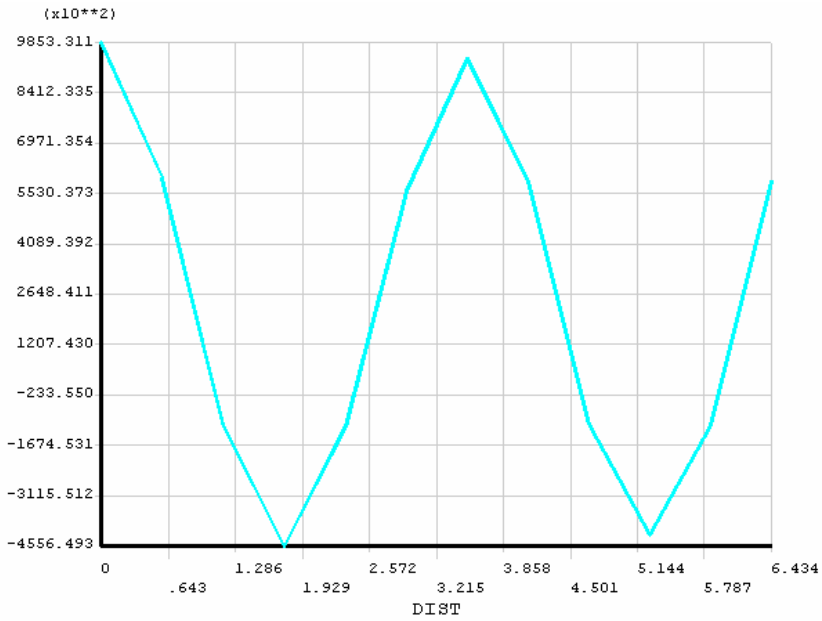


**Figure 18** The first principal stress change curve of path under case 2(Pa) (see online version for colours)

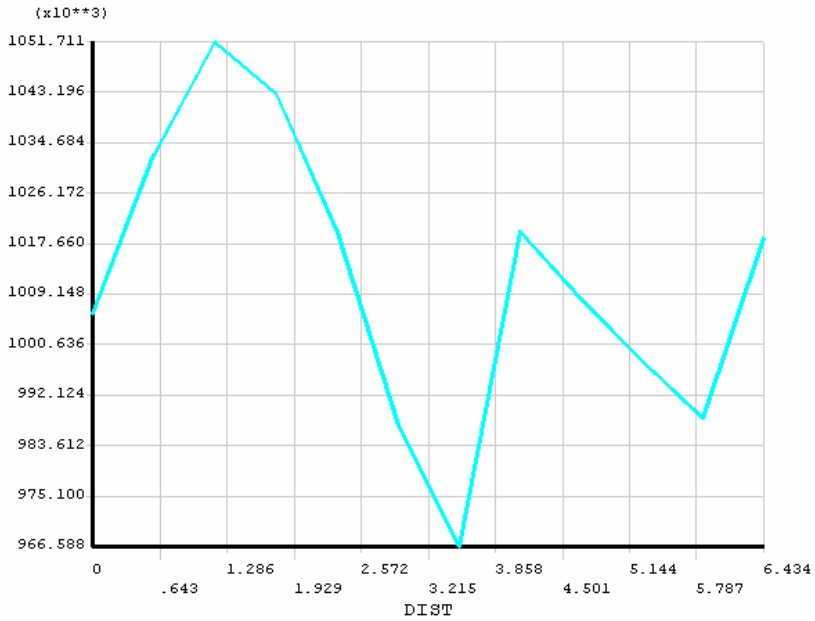


**Figure 19** The transverse stress change curve of path under case 3(Pa) (see online version for colours)

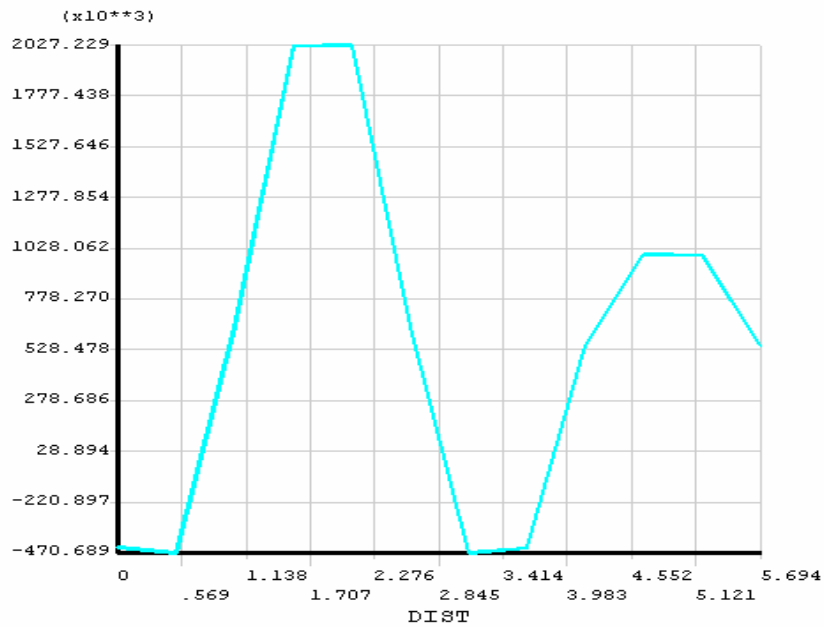


**Figure 20** The first principal stress change curve of path under case 3(Pa) (see online version for colours)

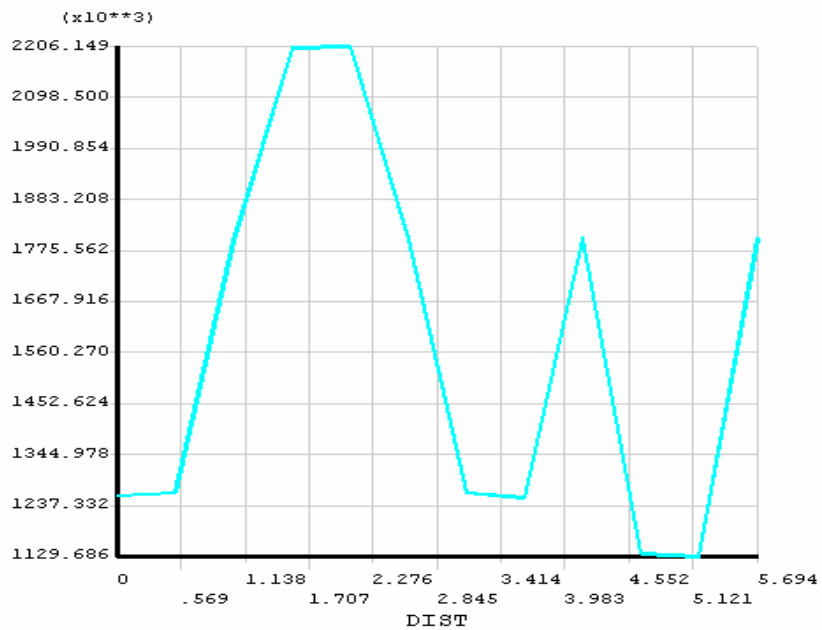


**Figure 21** The transverse stress change curve of path under case 4(Pa) (see online version for colours)

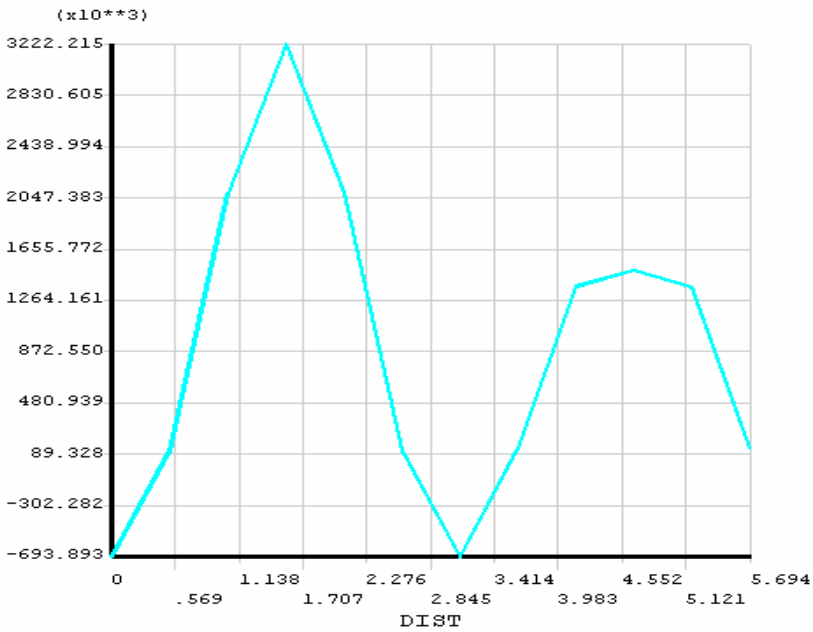
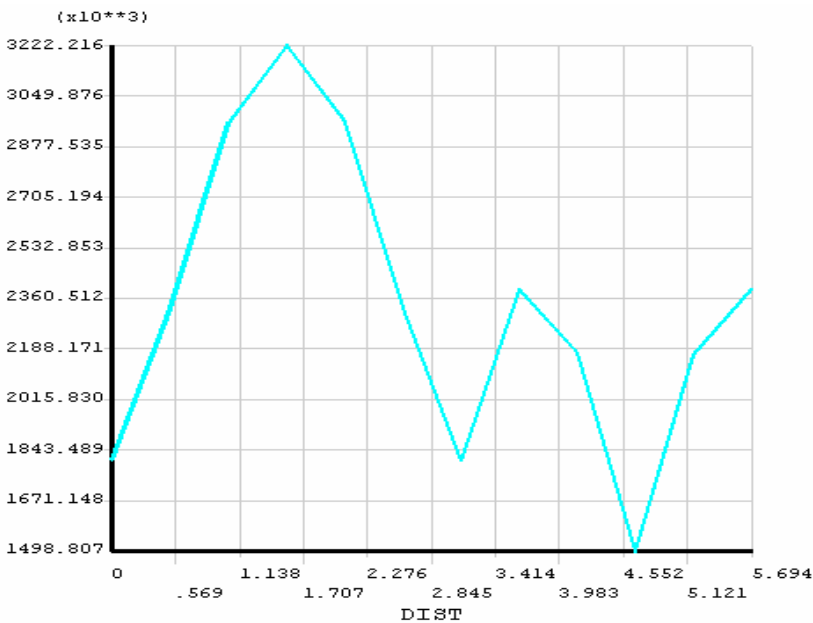


**Figure 22** The first principal stress change curve of path under case 4(Pa) (see online version for colours)



As can be seen from the stress change curve on the path under various cases, from case 1 to case 4, with the application of prestress and the increase of water pressure, the



transverse stress of the inverted siphon is small and gradually increases. The maximum is achieved under the combined action of the structural weight, prestress and design water pressure, when the inverted siphon structure is designed, it can be used as the design basis to check the structural safety. The maximum tensile stress of inverted siphon reaches 3.22 MPa, which is greater than the tensile strength of C30 concrete, but only in the small area of the inverted siphon, it is the elbow joint, and here there is a pier to fix it, with stirrups inside, the safety of inverted siphon structure is evaluated comprehensively, which meets the design requirements.

### 4.3 Displacement cloud map

By analysing the deformation of the trench embedded prestressed inverted siphon structure, the displacement distribution cloud map of inverted siphon structure under two cases is obtained, they are shown from Figure 23 to Figure 26.

As can be seen from the deformation analysis results of the inverted siphon structure, under case 1, the maximum vertical displacement of the inverted siphon is 0.04 mm, which appears at the end of the inverted siphon; The maximum lateral displacement was 0.01 mm, which appeared at the intersection of the oblique straight section and the horizontal section of the inverted siphon. Under case 4, the maximum displacement of the inverted siphon is 0.15 mm, which appears at the intersection of the oblique straight section and the horizontal section of the inverted siphon; The maximum lateral displacement is 0.15 mm, which appears at the intersection of the oblique straight section and the horizontal section of the inverted siphon. The overall displacement of the inverted siphon is very small, which can meet the design requirements.

**Figure 23** The vertical displacement cloud map of inverted siphon under case 1(m) (see online version for colours)

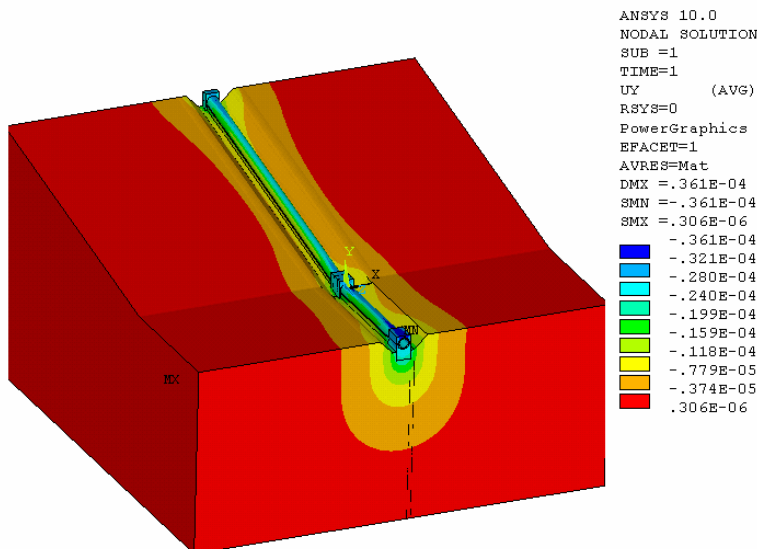


**Figure 24** The transverse displacement cloud map of inverted siphon under case 1(m) (see online version for colours)

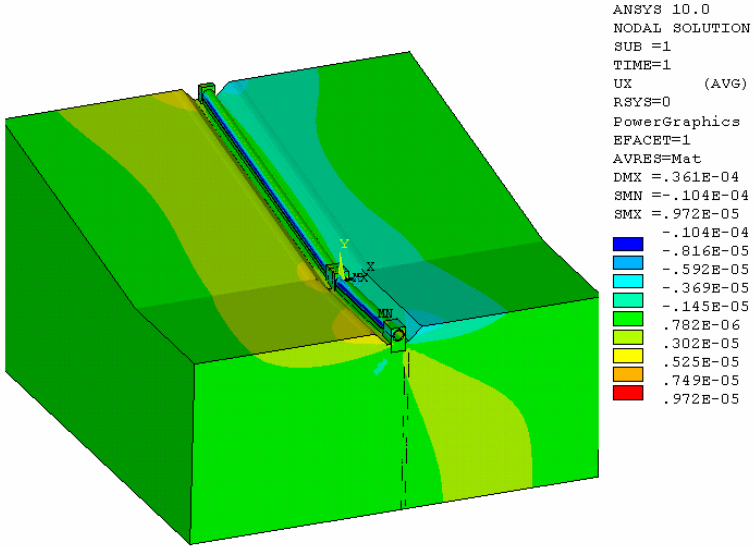


**Figure 25** The total displacement cloud map of inverted siphon under case 4(m) (see online version for colours)

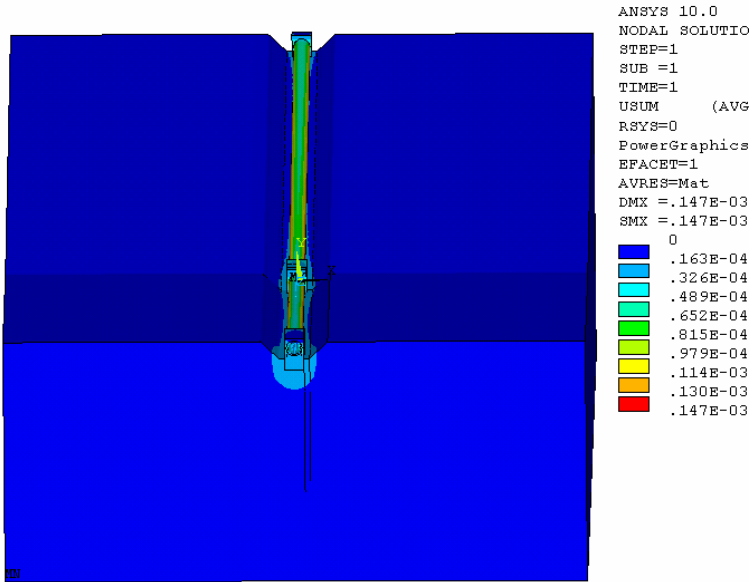
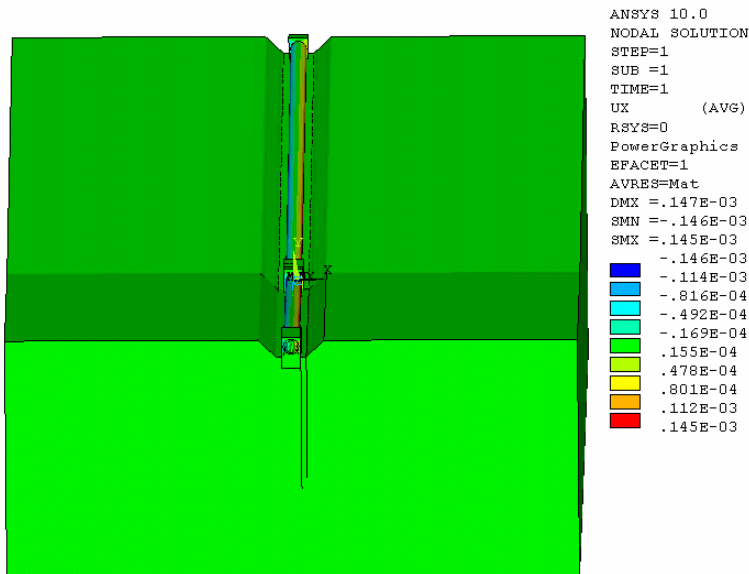


**Figure 26** The transverse displacement cloud map of inverted siphon under case 4(m) (see online version for colours)



## 5 Conclusions

To sum up, under the action of prestressed steel bar, the stress and displacement of inverted siphon are reduced, inverted siphon can withstand greater internal water pressure, effectively increase the safety of inverted siphon. The maximum tensile stress of inverted siphon structure is 2.26 MPa, which occurs in case 3, however, the stress distribution range is very small and belongs to local stress concentration. Under the design water pressure, the maximum circumferential tensile stress of prestressed reinforcement is 1310 MPa, which meets the requirements of tensile strength of reinforcement. The maximum vertical displacement of inverted siphon structure is 0.15 mm, which is very small and meets the design requirements. It can be seen that the design scheme of the buried inverted siphon structure is reasonable.

## References

- Fu, H., Guo, X.L., Yang, K.L., Wang, T. and Guo, Y.X. (2017) 'Ice accumulation and thickness distribution before inverted siphon', *Journal of Hydrodynamics*, Ser. B, No. 2, pp.61–67.
- Hu, R.H. and Zhang, W.L. (2004) *Hydraulic Structure*, pp.12–16, People's Communications Press, Beijing.
- Ji, D.Y. (2010) 'Design and calculation of Gully-buried inverted siphon', *Water Conservancy Science and Technology and Economy*, Vol. 16, No. 8, pp.880–881.
- Li, C.Y. (2018) 'Calculation and application of internal force of inverted siphon', *Heilongjiang Hydraulic Science and Technology*, Vol. 46, No. 9, pp.155–157, 204.

- Li, H.Y., Tian, W.D., Yan, H.X. (2006) *Inverted Siphons*, pp.19–23, China Water Conservancy and Hydropower Press, Beijing.
- Liu, K.D. (2016) ‘Application of finite element method in prestressed trench buried inverted siphon analysis’, *Heilongjiang Science and Technology Information*, Vol. 16, No. 8, pp.123–124.
- Niu, J., Ji, R.C. and Niu, H.Y. (2018) ‘Analysis of box inverted siphon structure’, *Gansu Water Resources and Hydropower Technology*, Vol. 54, No. 1, pp.26–28.
- Peng, L.W. (2019) ‘Stability monitoring and analysis in operation period of a water diversion siphon project’, *Shaanxi Water Resources*, No. 1, pp.180–181.
- Ren, C. (2003) *Practical Analysis Tutorial of ANSYS*, pp.32–36, Peking University Press, Beijing.
- SL191-2008 (2008) *Design Code for Hydraulic Concrete Structure*, pp.22–25, China Water Conservancy and Hydropower Press, China.
- Wang, J.H., Chen, C., Li, S.S. and Du, Y. (2018) ‘Safety analysis of the inverted siphon of the Yongding River based on three dimensional finite element method’, *Beijing Water*, No. 5, pp.23–26.
- Wang, X.C. (2003) *Finite Element Method*, pp.82–87, Tsinghua University Press, Beijing.
- Zhang, H. (2018) ‘Several problems should be paid attention to in the design of inverted siphon’, *Sichuan Water Resources*, No. 4, pp.49–51.
- Zhao, Y.B. (2018) ‘Review and analysis of inverted siphon flood control in the channel of south-to-north water diversion project’, *Henan Water Resources and South-to-North Water Diversion*, No. 8, pp.41–44.
- Zheng, T.L. and Ma, J.H. (2019) ‘Transformation of inverted siphon of canal in fushi irrigation area’, *Small Hydro Power*, No. 1, pp.49–65.